

# Body Motion for Powering Biomedical Devices

Edwar Romero, Robert O. Warrington, and Michael R. Neuman, *Senior Member, IEEE*

**Abstract**—Kinetic energy harvesting has been demonstrated as a useful technique for powering portable electronic devices. Body motion can be used to generate energy to power small electronic devices for biomedical applications. These scavengers can recharge batteries, extending their operation lifetime or even replace them. This paper addresses the generation of energy from human activities. An axial flux generator is presented using body motion for powering miniature biomedical devices. This generator presents a gear-shaped planar coil and a multipole NdFeB permanent magnet (PM) ring with an attached eccentric weight. The device generates energy by electromagnetic induction on the planar coil when subject to a changing magnetic flux due to the generator oscillations produced by body motion. A 1.5 cm<sup>3</sup> prototype has generated 3.9 μW of power while walking with the generator placed laterally on the ankle.

## I. INTRODUCTION

Energy harvesting is a research area that has lately gained attention for powering portable electronic devices. Considering that electronic biomedical devices are restricted by battery size and limited life time, energy harvesting can be an interesting option to reduce the number of surgeries associated with battery replacement, decreasing health care costs and patient discomfort. For instance, cardiac pacemakers have an average lifetime of 5-12 years depending on the pacemaker type [1].

Human activities have been considered as energy sources for harvesting either using electromagnetic, piezoelectric, or electrostatic transduction methods [2][3]. The literature tends to slightly favor the use of electromagnetic energy generation for this application because of its higher power output [3][4]. The relatively high impact forces generated while walking has attracted interest for heel-strike generators using piezoelectric and electrostatic devices [5] with power outputs in the order of few mW. Inertial forces, varying from several grams (few cm<sup>3</sup>) to several pounds (hundreds of cm<sup>3</sup>), have also been employed for energy generation either inside shoes [6] or backpacks [7] with power ranging correspondingly

from few milliwatts to a few watts. Traditional research has been focused on power generation without considering desirable human body locations and their energy availability. Only [8] has presented an overview of possible locations according to the work performed at the joints while walking. Meanwhile, this work suggests how much power can be harvested for given body locations from human walking.

Our research has been concentrated on unobtrusive energy harvesting and estimation of available power from human activities. The induced accelerations on the ankle, knee, wrist, elbow, shoulder, and head during walking have been analyzed and power has been estimated. Devices have been built in order to harness the available energy from the body using electromagnetic induction.

Most energy harvester designs present large generators based on a restricted linear displacement of a proof mass, but human motions are not linear and not restricted. Therefore, traditional scavengers are challenged by body motion. The design presented here is for an unobtrusive generator with a volume in the order of 1cm<sup>3</sup>. The generator proposed is based on a rotational mechanism (non-resonant conversion) similar to the one traditionally found on a self-winding wristwatch, which is well suited for human motion. In addition to the successful self-winding wristwatch design, no other generator using a rotational approach has been employed as an energy source for powering biomedical devices. In this paper the estimation of available energy from human walking and the development of an axial flux generator harvesting human motion are described.

## II. AVAILABLE POWER

Power generation from energy harvesters is proportional to the proof mass ( $m$ ), the acceleration ( $a$ ) squared, and the quality factor ( $Q$ ) and inversely proportional to the driving frequency ( $\omega$ ) for a system where the driving frequency matches its resonant frequency:

$$P = \frac{1}{2} m \frac{a^2}{\omega} Q \quad (1)$$

Therefore, larger ratios of acceleration-squared-to-frequency ( $ASTF$ ) and larger  $Q$  factors are related to a higher available power. Human body motion belongs to the category with large  $ASTF$  values and low  $Q$  factors, while machines are typically associated with the opposite. Romero *et al.* [9] estimated that human motion could produce as much power as 1 mW/cm<sup>3</sup> from walking. This level of

Manuscript received April 7, 2009. This work was supported by the National Science Foundation under Award Number EEC-0096866.

E. Romero is with the Mechanical Engineering Department, Michigan Technological University, Houghton, MI 49931, on leave from the Mechanical Engineering Department, Turabo University, Gurabo, PR 00778 USA (phone: 906-487-2551; fax: 906-487-2822; e-mail: eromero@suagm.edu).

R. O. Warrington is with the Mechanical Engineering Department, Michigan Technological University, Houghton, MI 49931 (e-mail: row@mtu.edu).

M. R. Neuman is with the Biomedical Engineering Department, Michigan Technological University, Houghton, MI 49931 (e-mail: mneuman@mtu.edu).

power makes it possible to energize low-power applications, either by charging batteries or used instead of batteries.

To estimate how much power is available for energy harvesting, the *ASTF* parameter needs to be known. Acceleration was measured for walking in order to determine body locations with high *ASTF* values. Acceleration was recorded on three subjects at several locations under normal gait. This was performed using a wireless sensor network (WSN) mote (Sun SPOT). Measured acceleration and frequency values on Table I are considered to be in accordance with those found during locomotion studies [10].

TABLE I  
ASTF FACTORS FOR HUMAN WALKING.

Location	Acceleration <sup>a</sup> (G's)	Frequency (Hz)	ASTF
Ankle	2.5-2.7	1.0-1.7	50-120
Knee	1.7-2.0	1.7-2.0	20-70
Hip	0.4-0.8	1.7-2.0	1-5
Wrist	0.3-0.5	1.0-1.7	1-4
Elbow	0.3-0.5	1.2-2.0	1-2
Shoulder	0.3-0.4	1.7-2.0	~1
Chest	0.3-0.4	1.7-2.0	~1
Back of the head	0.4-0.7	0.8-2.0	1-8

<sup>a</sup>1G = 9.8 m/s<sup>2</sup>

An electromagnetic energy harvester has a maximum power transfer to the electrical load close to 50% of the power flowing into the device [11]. The estimated power output is then presented in Fig. 1, assuming a modest *Q* factor of 1 and choosing several proof mass sizes. Therefore, a device in the order of 1cm<sup>3</sup> having a 1 g proof mass could produce several mW of raw power if placed on the ankle or knee, or hundreds of  $\mu$ W for less energetic locations.

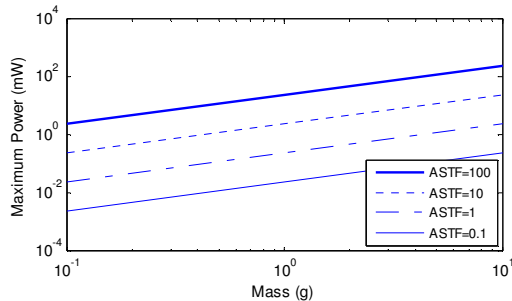


Fig. 1. Maximum power generation for an electromagnetic energy harvester with a *Q* factor of 1.

### III. DEVICE OPERATION AND DESIGN

A 3D schematic of the prototype generator for body motion is shown in Fig. 2. This generator uses the motion conversion mechanism for body movements found in automatic self-winding wristwatches (rotations or oscillations due to the unbalanced proof mass), and employs the approach of axial flux generators used in small-scale wind turbines (multiple pole-pairs arrangements of permanent magnets and coils). The rotor is composed of two rings with multiple pole-pairs of NdFeB permanent magnets (PM) and an eccentric mass. The stator is made of several stacked layers of a gear-shaped planar coil fabricated using

thin-film technology. The gear-shaped planar coil is used because it simplifies the wiring to two electrical connections per layer. Body movement provides the driving force needed to move the rotor eccentric mass. Once this mass is perturbed it oscillates behaving as a pendulum. Hence, the variation of the magnetic field due to the rotor oscillations induces a voltage on the planar coil according to Faraday's Law of Induction. This AC output voltage is later rectified into a DC signal and stored in a capacitor or rechargeable battery for later use. Since the device operation and fabrication resembles the one found in self-winding wristwatches, it is estimated that the generator can present a long life and maintenance-free operation for implantable devices, such as cardiac pacemakers, cochlear implants, body sensor networks, and neural and muscle stimulation devices.

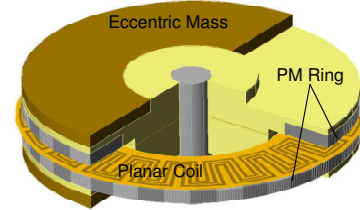


Fig. 2. 3D schematic of the axial flux generator.

The simplified diagram for the induced voltage analysis for a one pole-pair coil is presented in Fig. 3. A magnetic field distribution of the vertical component with a simplified sinusoidal shape wave per pole-pair was assumed ( $B = B_r \sin(\theta_p)$ ), where  $\theta_p$  is the angle per pole-pair. The generator is analyzed with an oscillating angular velocity  $\omega$ . Voltage is only induced on the radial segments of the planar coil; therefore no voltage is induced on the arc shaped segments. Fleming's right-hand rule was used for the representation of the induced current. The planar coil was fabricated with identical radial lengths to simplify the analysis. The relation for the induced voltage across the planar coil with *N* turns per coil and *p* number of poles is expressed as:

$$V_o = -N p \omega (r_1 + r_2) l B_r \sin(\theta_p) \quad (2)$$

The generated power is calculated using the internal coil resistance  $R_c$  and the load resistance  $R_L$  as:

$$P_o = V_o^2 / (R_C + R_L)^2 R_L \quad (3)$$

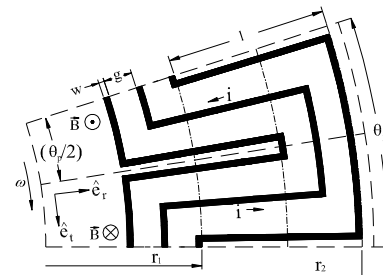


Fig. 3. Induced voltage analysis for one pole-pair segment.

Since it is difficult to match the device resonant frequency to the driving frequency of body motion, the generator will not be able to produce the energy level estimated in Fig. 1. A 25 mm diameter generator with a 1g mass has been found to have a resonant frequency of 2.8 Hz, and subharmonics at 1.5 and 1 Hz. This is evidenced in Fig. 4 from the test results on a laboratory shaker. Although the resonant frequency is not close to the values presented in Table I, its subharmonics are. Otherwise, a generator with a diameter in excess of 100mm would be required. Although a higher power output is observed at the resonant frequency, about a third of the maximum power was produced at 1.5 Hz, and close to a tenth at 1 Hz. This leaves an estimated power of 10-30% of the maximum available for driving frequencies respectively of 1 and 1.5 Hz. Human walking frequency is close to 1 Hz, thus this type of generator could be able to harvest 10% of the maximum available power (on the order of hundreds of microwatts).

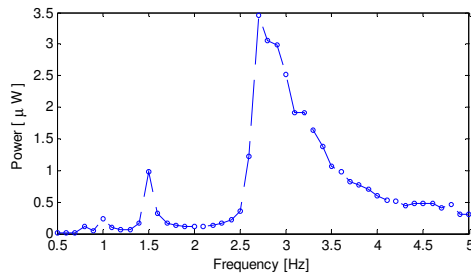


Fig. 4. Power output produced with the generator tested on a laboratory shaker. 10-layer coil (200  $\mu\text{m}$  linewidth and 4 turns) and 20 discrete NdFeB PM pole-pairs (2 mm x 1 mm x 1mm).  $R_{\text{load}}=44 \Omega$ ,  $R_{\text{coil}}=44 \Omega$ ,  $V_{\text{RMS}}=24.6 \text{ mV}$ ,  $P=3.5 \mu\text{W}$ .

Although operation at resonant frequencies provides higher power output, this generator is not limited to operate at resonance as resonant devices do. Human walking and human activities have a broad frequency spectrum where a fixed-frequency generator would be extremely limited. The non-resonant conversion design presented here, the rotational mechanism, is not limited to operate at a small frequency bandwidth. Inertial forces from body movement play an important role providing the kinetic energy needed to start the generator oscillations, in the same fashion as self-winding wristwatches oscillate by body movements.

The design objective for this generator was to harvest as much energy as possible while having a small size. Equation (2) helps to identify the parameters to be optimized: coil dimensions, number of pole-pairs, coil turns, and PM remanence (a NdFeB PM was chosen due to its high remanence). These variables should be as high as possible under a given size constraint while minimizing at the same time the winding losses. Therefore a tradeoff between a small coil linewidth and a large number of poles is made. A configuration with a single PM ring rotor placed in between two stators doubles the planar coil windings, and a stator placed in between two PM rings increases the PM remanence. These two design configurations promise a

higher voltage output that ensures a higher generated power. Coil linewidth size is limited by the photoplotter resolution on the actual prototypes. The simulation parameters are presented in Table II. Fig. 5 shows a simulation of the induced open-circuit peak voltage for 1-layer coil with a proof mass released at  $45^\circ$  from the vertical position (no damping was assumed for this model). Fig. 5 also shows the results of the induced voltage output for two tests employing a 100  $\mu\text{m}$  and a 200  $\mu\text{m}$  planar coil with a pendulum mass released at  $45^\circ$ .

TABLE II  
SIMULATION PARAMETERS.

Parameter	Value
Generator area	491 mm <sup>2</sup>
Generator volume	1.5 cm <sup>3</sup>
Coil outer diameter	25 mm
Coil inner diameter	21 mm
Coil linewidth	200 $\mu\text{m}$
Coil linewidth spacing	100 $\mu\text{m}$
Coil turns per layer	4
Coil resistance per layer	4.3 $\Omega$
Pole-pairs	20
PM material	NdFeB (Grade N35)
PM thickness	1.1 mm
PM size	5.1 mm x 1.1 mm x 1.1 mm
Airgap thickness	1 mm

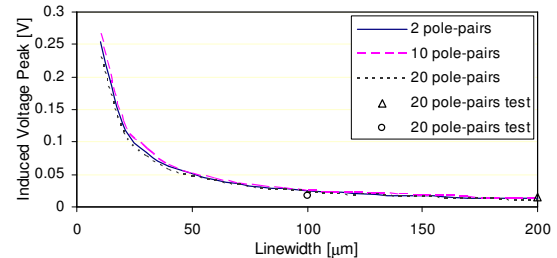


Fig. 5. Induced open-circuit peak voltage simulation per layer for a 1 g pendulum mass released at  $45^\circ$  under varying linewidth and pole-pair number (No damping was assumed for this model). 2 tests for a 100  $\mu\text{m}$  (9 turns) and a 200  $\mu\text{m}$  (4 turns) linewidth single layer coil with 20 discrete NdFeB PM pole-pairs (2 mm x 1 mm x 1mm) are included.

#### IV. FABRICATION, TESTING AND DISCUSSION

The main components of the generator, as shown in Fig. 2, are the rotor and the stator. The rotor was fabricated with 20 discrete (5.1 mm x 1.1 mm x 1.1 mm) pole-pairs of NdFeB PM (grade N35) placed into a 25 mm diameter slotted PMMA disc. The rotor was attached to a 1 g eccentric mass, fitted with a steel spindle, and packaged in a PMMA package. Sapphire jewel bearings were used to finalize the 1.5 cm<sup>3</sup> generator assembly. The planar coil is shown in Fig. 6. The planar-coil internal electrical resistance was calculated as 4.4  $\Omega$  and was measured as 4.9  $\Omega$ ; this difference is explained by copper undercut when etching as observed by photographic analysis.

The generator was tested on the limbs of an individual while walking. The output voltage for the ankle location is shown in Fig. 7, where the peak voltage and peak power

were respectively 59.4 mV and 44  $\mu$ W for a 2-layer (200  $\mu$ m linewidth coil and 4 turns). No  $Q$  factor was measured to estimate the actual available power, according to (1). But the efficiency of the actual generator is relatively low,  $\sim 4\mu$ W out of  $\sim 100\mu$ W, for the tested prototype. Further designs should allow higher efficiencies, and therefore higher power outputs.



Fig. 6. Photo of a 200  $\mu$ m linewidth planar coil etched on a copper-clad polyimide film (25  $\mu$ m thick polyimide, 18  $\mu$ m thick copper, 25 mm diameter, 4 mm radial linewidth length).

Preliminary tests showed that generators placed on the lower limbs are capable of producing a higher power output. Only two locations were evaluated with a matching load, the other locations were evaluated for open-circuit output voltage, as shown in Table III. According to Table III the device was able to generate a higher amount of power when placed on the ankle while walking, as expected from the *ASTF* relation.

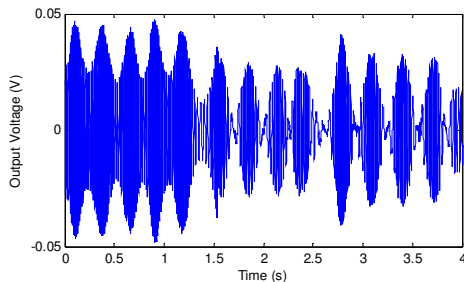


Fig. 7. Voltage output generated while walking with generator placed laterally on the ankle for a 2-layer coil (200  $\mu$ m linewidth and 4 turns) and 20 discrete NdFeB PM pole-pairs (5.1 mm x 1.1 mm x 1.1 mm).  $R_{load}=10 \Omega$ ,  $R_{coil}=9.8 \Omega$ ,  $V_{RMS}=17.6$  mV,  $P=3.9 \mu$ W.

TABLE III  
GENERATOR RESULTS WHILE WALKING.

Location	Peak Voltage (mV)	Voltage (mV <sub>RMS</sub> )	Average Power ( $\mu$ W)
Elbow	26.6	7.9	-
Wrist	8.6	1.7	-
Hip	23.8	9.3	-
Knee	46.6	15.4	3.0
Ankle	59.4	17.6	3.9

Energy harvesters placed on the lower limbs were found to produce higher power levels due to the larger *ASTF* factors in comparison with upper limbs and other body locations. Following Table I, lower limbs have *ASTF* factors as high as 10 times larger than those from upper limbs, thus according to (1) lower limb locations can outpace upper limbs for a factor of 10.

Due to fabrication constraints, prototype generators with a

low number of layers and coil density were employed. Therefore, further designs presenting a larger number of layers with high density coils are expected to increase significantly the power produced. Voltage output for an energy harvester needs to be at higher levels than semiconductor p-n junction threshold voltages in order to use solid state diode rectification ( $> 200$ mV). A larger number of layers with higher density coils are expected to produce a 10 fold increase in the generated voltages ( $> 500$  mV) on later prototypes. A power-management circuit composed of a voltage multiplier (to increase and rectify the generated voltage) and a capacitor (to store the energy) allows the generation of useful DC voltages as presented by [12].

## V. CONCLUSION

The design of energy harvesters for implantable biomedical devices driven by body motion can make hybrid designs (rechargeable battery + scavenger) plausible. This approach can enhance the service life of battery operated devices decreasing the need of periodic patient surgery, lessening the associated health care cost, and patient discomfort. Energy generation from body activities is a valid technique to energize implantable devices. Careful design should account for the available energy from a given body location for a harvester intended to power an electronic device.

## REFERENCES

- [1] D. Katz and T Akiyama, "Pacemaker longevity : The world's longest-lasting VVI pacemaker", *Annals of Noninvasive Electrocardiology*, 2007, vol. 12, N. 3, pp 223 – 226.
- [2] T. Stamer, "Human-Powered wearable computing", *IBM Systems Journal*, 1996, vol. 35, pp. 618-629.
- [3] E. Romero, R. O. Warrington and M. R. Neuman, "Energy scavenging sources for biomedical sensors", *Physiological Measurement*, submitted for publication.
- [4] S. P. Beeby, M. J. Tudor, and N. M. White, "Energy harvesting vibration sources for microsystems applications", *Meas. Sci. Technol.* 2006, Vol. 17, pp. R175–R195.
- [5] T. Starner and J. A. Paradiso, "Human Generated Power for Mobile Electronics" in *Low-Power Electronics Design*, C. Piguert, Ed. Boca Raton: CRC Press, 2004.
- [6] M. Duffy and D. Carroll, "Electromagnetic generators for power harvesting", *PESC 2004*, vol. 3, pp. 2075-2081.
- [7] L. C. Rome, L. Flynn, E. M. Goldman, and T. D. Yoo, "Generating Electricity While Walking with Loads", *Science*, 2005, vol. 309, pp. 1725-1728.
- [8] P. Niu, P. Chapman, R. Riemer, and X. Zhang, "Evaluation of motions and actuation methods for biomechanical energy harvesting", *PESC 2004*, vol 3, pp 2100-2106.
- [9] E. Romero *et al.*, "Micro energy scavengers", *Electronic Proc. COMS 2008*.
- [10] E. Hirasaki, S. T. Moore, T. Raphan, and B. Cohen, "Effects of walking velocity on vertical head and body movements during locomotion", *Experimental brain research*, 1999, vol. 127, pp. 117-130.
- [11] N. G. Stephen, "On energy harvesting from ambient vibration", *J. of sound and vibration*, 2006, vol. 293, pp. 409-42
- [12] J. M. H. Lee, S. C. L. Yuen, W. J. Li, and P. H. W. Leong, "Development of an AA Size Energy Transducer with Micro Resonators", *ISCAS '03*, vol. 4, pp. 876-9.